The Journal of Chemical Physics

Surface potential of liquid microjet investigated using extreme ultraviolet photoelectron spectroscopy

Cite as: J. Chem. Phys. **152**, 144503 (2020); https://doi.org/10.1063/5.0005930
Submitted: 27 February 2020 . Accepted: 23 March 2020 . Published Online: 13 April 2020

Junichi Nishitani, Shutaro Karashima, Christopher W. West, and Toshinori Suzuki

The Journal of Chemical Physics ARTICLE scitation.org/journal/jcp

Surface potential of liquid microjet investigated using extreme ultraviolet photoelectron spectroscopy

Cite as: J. Chem. Phys. 152, 144503 (2020); doi: 10.1063/5.0005930
Submitted: 27 February 2020 • Accepted: 23 March 2020 •
Published Online: 13 April 2020

Junichi Nishitani, Shutaro Karashima, Christopher W. West, and Toshinori Suzuki[a)]

AFFILIATIONS

Department of Chemistry, Graduate School of Science, Kyoto University, Kitashirakawa-Oiwakecho, Sakyo-Ku, Kyoto 606-8502, Japan

[a)]Author to whom correspondence should be addressed: suzuki@kuchem.kyoto-u.ac.jp

ABSTRACT

Photoelectron spectroscopy of a liquid microjet requires careful energy calibration against electrokinetic charging of the microjet. For minimizing the error from this calibration procedure, Kurahashi *et al.* previously suggested optimization of an electrolyte concentration in aqueous solutions [Kurahashi *et al.*, J. Chem. Phys. **140**, 174506 (2014)]. More recently, Olivieri *et al.* proposed an alternative method of applying a variable external voltage on the liquid microjet [Olivieri *et al.*, Phys. Chem. Chem. Phys. **18**, 29506 (2016)]. In this study, we examined these two methods of calibration using extreme ultraviolet photoelectron spectroscopy with a magnetic bottle time-of-flight photoelectron spectrometer. We confirmed that the latter method flattens the vacuum level potential around the microjet, similar to the former method, while we found that the applied voltage energy-shifts the entire spectrum. Thus, careful energy recalibration is indispensable after the application of an external voltage for accurate measurements. It is also pointed out that electric conductivity of liquid on the order of 1 mS/cm is required for stable application of an external voltage. Therefore, both methods need a similar concentration of an electrolyte. Using the calibration method proposed by Olivieri *et al.*, Perry *et al.* have recently revised the vertical ionization energy of liquid water to be 11.67(15) eV [Perry *et al.*, J. Phys. Chem. Lett. **11**, 1789 (2020)], which is 0.4 eV higher than the previously estimated value. While the source of this discrepancy is still unclear, we estimate that their calibration method possibly leaves uncertainty on the order of 0.1 eV.

I. INTRODUCTION

Photoelectron spectroscopy using a liquid microjet technique provides invaluable insights into the electronic structure and dynamics of liquids.[1–18] However, the method requires careful energy calibration owing to spontaneous electric charging of the microjet.[19–25] When Faubel and colleagues pioneered the microjet technique, they had already recognized a strong electrokinetic charging effects and argued that photoelectron spectroscopy of microjets requires the addition of an electrolyte or adjustment of pH to suppress the charging.[26] Later, we found that photoelectrons are accelerated or decelerated by the microjet, depending on the electrolyte concentration, and we found the best concentration that eliminates the influence of electrokinetic charging to be about 30 mM for NaX (X = Cl, Br, and I).[22] A similar result has also been reported by Preissler and co-workers.[23] Alternatively, Olivieri and co-workers proposed the manipulation of the electric potential of a microjet by applying an external voltage to obtain a similar effect with the adjustment of electrolyte concentration.[27] In the present study, we investigate both methods by extreme UV (XUV) photoelectron spectroscopy with a magnetic bottle time-of-flight (MBTOF) electron spectrometer[28] to find a reliable protocol for measurements.

Photoelectron spectroscopy measures the kinetic energy distribution of electrons emitted from a sample and determines the electron binding energy (eBE) of a material and/or an electronic state of interest. eBE is calculated from the difference between the photon energy and the photoelectron kinetic energy (PKE). For accurate measurements of PKE, a photoelectron spectrometer must be carefully energy-calibrated using a standard sample for which

accurate eBE is known, for example from spectroscopic studies of Rydberg series or pulsed field ionization zero kinetic energy (PFI-ZEKE) spectroscopy.[29,30] However, when a liquid microjet is introduced into a spectrometer, the electric potential changes and energy recalibration become necessary.

In energy recalibration using a reference gas, the ionization point of the gas is spatially close to, yet not exactly at the liquid. Since the Coulombic potential rapidly changes at short distances, extrapolation from the nearest measurement point to a shorter distance becomes necessary.[21,22] For minimizing the error arising from this extrapolation, it is desirable to avoid a steep potential (or vacuum energy level) gradient around the microjet; a steep slope causes a greater error in the extrapolation. Figure 1(a) illustrates the situation of potentials in a typical MBTOF spectrometer. The ionization region is located between a strong permanent magnet [e.g., samarium–cobalt (SmCo)] and an entrance skimmer (aperture) of a time-of-flight (TOF) electron energy analyzer, both of which are coated with graphite. The symbols Φ_g and Φ_{an} are the work functions of graphite and the analyzer, respectively. The Fermi levels (E_F) of the magnet, liquid, skimmer, and analyzer at equilibrium are equal, whereas the local vacuum energy levels (E_{vac}) are different owing to the differences in their work functions determined by electronic structures of materials and surface conditions. In this figure, E_{vac} of the liquid is assumed to be higher than E_{vac} of graphite so that the photoelectron is accelerated during its flight from the liquid to the skimmer. Photoelectrons emitted from the reference gas molecules in the ionization region will have different kinetic energies owing to the vacuum level gradient between the liquid and the skimmer.

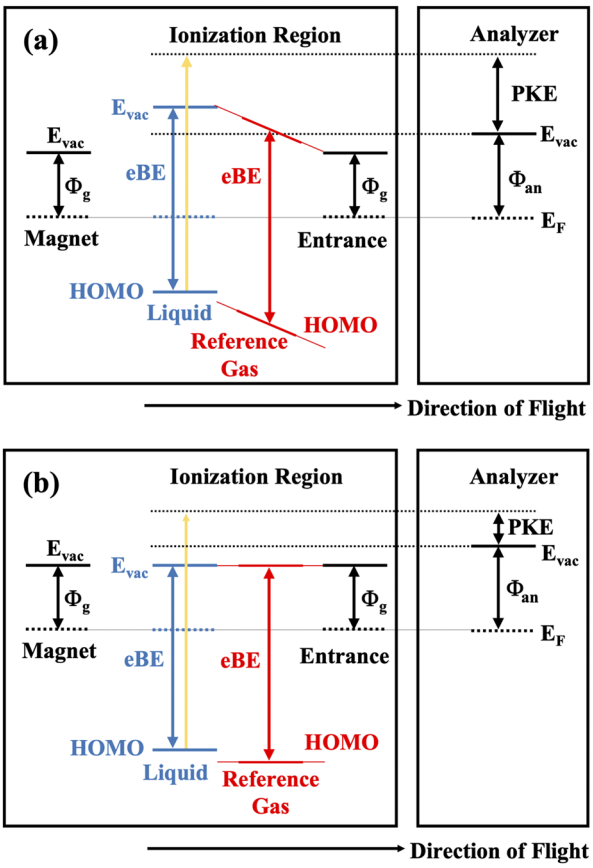

FIG. 1. Electronic energies of the relevant components in a magnetic bottle photoelectron spectrometer in which the magnet and the entrance skimmer for the energy analyzer are graphite coated. Vacuum level of liquid is higher than that of graphite in (a) and equal to in (b).

Figure 1(b) shows a more favorable experimental condition in which the composition of the liquid (the concentration of solutes) is adjusted so as to align the vacuum level of the liquid with respect to graphite. Then, PKE from a reference gas around the jet becomes independent of the ionization position, which makes the energy calibration to be considerably more straightforward. One can find a specific electrolyte concentration that makes PKE to be independent from the ionization position around the liquid microjet. As mentioned earlier, in the case of microjets of aqueous NaX (X = Cl, Br, and I) solutions discharged from a fused silica capillary with a 25 μm inner diameter at a flow rate of 0.5 ml/min, this specific concentration occurs at around 30 mM.[22] Therefore, this solute concentration has often been employed in photoelectron spectroscopy of liquids. The sample concentration can be varied easily using a gradient flow HPLC (high-performance liquid chromatography) pump, which mixes two solutions with any arbitrary ratio during the measurements. It is noted that, even if E_{vac} is flat in the ionization region, it can be different from E_{vac} in the analyzer. For example, in Fig. 1, Φ_{an} is assumed to be greater than Φ_g, which makes E_{vac} in the analyzer to be greater than that of the ionization region, so that electrons are decelerated when they enter the analyzer. Even when the inner surface of the analyzer is coated with graphite, the vacuum level in the analyzer can be raised by applying a negative voltage to the flight tube. This enables restriction of the observation energy region and rejection of low-energy background electrons. On the contrary, application of a positive voltage to the flight tube lowers the vacuum level, and it is useful for improving the transmission efficiency of low-energy electrons through the analyzer. In any case, the influence of the difference between Φ_g and Φ_{an} must be quantitatively evaluated as a calibration of the spectrometer. In our apparatus, the vacuum level of the analyzed can be varied by applying a variable voltage in order to change the electron pass energy. In what follows, we assume that such a basic calibration of the analyzer was already performed, and we exclude its discussion.

In Fig. 1, we have not indicated the influence of a liquid flow rate explicitly. Suppose that PKE observed for gaseous molecule around the jet diminishes as the liquid is moved away from the ionization point. It implies that the vacuum level is greater at the liquid than that at the graphite-coated vacuum components, as shown in Fig. 1(a). Since the instrument is electrically grounded, this is regarded as that the liquid is being negatively charged. In fact, Kurahashi *et al.* and Preissler *et al.* have experimentally confirmed that the electric potential and a streaming current of a liquid microjet are correlated.[22,23] On the other hand, PKE is generally influenced by work functions of the materials even without apparent electric charges. Therefore, in this study, we express the influence of the liquid on PKE as the difference of E_{vac} between the liquid and the graphite-coated skimmer. More explicitly, we define

Φ_{surf} as the difference of E_{vac} at the skimmer and at the liquid; $\Phi_{surf} = E_{vac}(skimmer) - E_{vac}(liquid)$. Thus, if E_{vac} is greater at the liquid than at the skimmer, Φ_{surf} takes a negative sign. When Φ_{surf} is zero, a photoelectron does not experience any potential gradient. With this definition, Φ_{surf} is practically compatible with the streaming potential discussed by Kurahashi *et al.*[22] In principle, Φ_{surf} may be divided into an offset potential (Φ_0) present at the zero flow rate and the additional potential (Φ_{stream}) dependent on the flow rate. However, we do not attempt their differentiation in the present study. Evaporation from the liquid surface brings some solvent and solute molecules into the gas phase; however, for simplicity of our discussion, we neglect the influence of electrically charged species evaporated from the liquid surface.[23]

As an alternative to the reference gas method described above, eBE of solvent water can also be used as a useful internal energy reference in photoelectron spectroscopy of aqueous solutions. Gaiduk *et al.*[31] performed benchmark calculations on the electronic structure of an aqueous 1M NaCl solution and compared their results with the experimental data measured by Kurahashi *et al.*[22] for the 0.03M aqueous NaCl solution. This comparison was questioned by Olivieri *et al.*, who argued that eBE of solvent water depends on the composition of aqueous solutions and that assumption of eBE invariant with the concentration is incorrect.[27] Thus, the concentration dependence of the photoelectron spectrum of solvent water was experimentally reexamined in detail by Pohl and co-workers, and they showed that eBE of solvent water in aqueous NaI solution varies only less than 150 ± 60 meV up to the concentrations as high as 8M.[32] Thus, they indicated that the eBE of solvent water is a useful energy reference in photoelectron spectroscopy of aqueous solutions. The vertical eBE of liquid water has been reported to be 11.16 eV,[11,34] 11.23 eV,[35] or 11.31 eV[22] by soft x-ray photoelectron spectroscopy using a hemispherical electron energy analyzer. The three experiments were technically almost identical; however, they differed by calibration against electrokinetic charging of the microjet. For example, Nishizawa *et al.*[35] employed 140 mM NaCl solution to perform their measurement, while Kurahashi *et al.* investigated the magnitude of electrokinetic charging as a function of NaX concentrations and determined eBE to be 11.31 eV; at the concentration of 140 mM of NaCl, the microjet is negatively charged, which leads to the underestimation of eBE. Thus, the key to accurate determination of eBE is the precise calibration against electrokinetic charging. Recently, Perry *et al.* have revisited the vertical eBE of liquid water to obtain 11.67(15) eV,[33] which is greater than the previous values by about 0.4 eV. This could be an important correction to one of the most useful energy standards in photoelectron spectroscopy of liquids; however, the origin of the rather large correction remains unclear. They applied a variable electric potential to the microjet, similar to the study of Olivieri *et al.*,[27] to flatten the vacuum potential around it. In the present study, we describe the importance of energy calibration after applying an external voltage to a microjet.

II. EXPERIMENTAL SECTION

A one-box Ti-sapphire regenerative amplifier (35 fs, 800 nm) with a repetition rate of 1 kHz or 10 kHz was used to produce XUV pulses. The fundamental (ω) or second harmonic (2ω) laser pulses were focused into a Kr gas cell using a quartz lens (f = 500 mm) and used to induce high harmonic generation (HHG). The 2ω laser pulses were produced with a 0.3 mm thick beta barium borate (BBO) crystal. Single order harmonic was isolated by using a pair of multilayer mirrors or a time-preserving monochromator. The schematic diagram of our experimental setup is illustrated in our previous reports.[36,37] In the ω-driving setup, the 19th order harmonic (19ω: 42 nm, 29.45 eV) was isolated using a coated mirror system.[36] As for the 2ω-driving setup, the 14th order (14ω: 57 nm, 21.7 eV) harmonic was selected using the grating system. The diameter of the XUV beam at the microjet was estimated to be about 50 μm and 100 μm FWHM using the mirror or grating system, respectively. The magnetic bottle collected more than 50% of the photoelectrons emitted from the sample to the detector. Photoelectrons were detected using a Chevron microchannel plate (MCP) with a 38-mm effective diameter and a preamplifier, and electron counts were measured using a multi-channel scaler.

In most of our experiments, we introduced a continuous liquid microjet into a photoionization chamber through a 25-μm inner diameter capillary at a flow rate of 0.5 ml/min. The microjet discharged from the nozzle generally undergoes disintegration within a traveling distance of 10 mm owing to the amplification of microscopic turbulence. In the present study, the disintegrated liquid droplets are collected with a liquid nitrogen-cooled trap so that no electron backstreaming can occur through the liquid microjet from the cold trap. Alternatively, one can collect the liquid microjet before its disintegration to recirculate the sample liquid; Riley and co-workers have argued that the liquid recirculation system reduces the electrokinetic charging effect significantly in comparison with the cold trap method.[38]

The work functions of materials around the ionization position influence PKE. Thus, it is a standard method in photoelectron spectroscopy to coat the vacuum components with graphite. As a precondition for our discussion described later, we examined the effectiveness of the graphite coat using the experimental geometry shown in Fig. 2 and photoionization of Xe atoms with the 21.7 eV probe photons. In this experimental geometry, the head of the iron

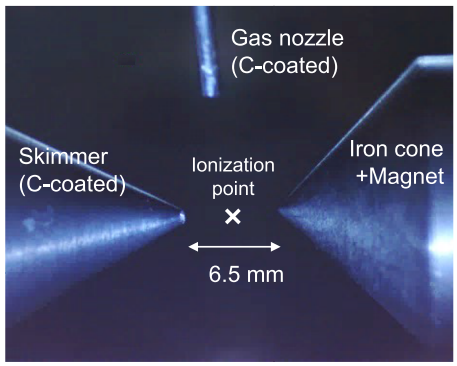

FIG. 2. Experimental geometry for studying the influence of materials around the ionization position (indicated by cross). The skimmer with an opening diameter of 0.5 mm and a gas nozzle made of PEEK were coated with graphite. The bottom of the iron cone is directly attached to a SmCo permanent magnet. The iron cone is coated with graphite or wrapped with an Al foil (see the text).

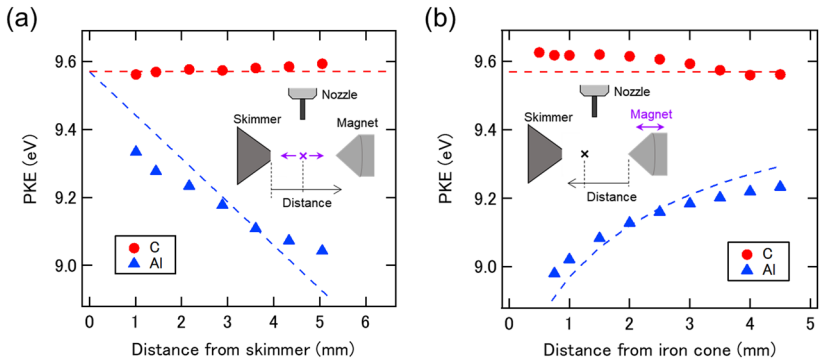

FIG. 3. Experimentally measured PKE associated with the $^2P_{3/2}$ Xe^+ band. The inset shows the experimental geometries. In all cases, the graphite-coated gas nozzle is placed more than 10 mm away from the ionization point (indicated by cross) to avoid its influence. Red dots are the results obtained with a graphite-coated iron cone on a SmCo magnet, and blue triangles are with an Al-wrapped iron cone. (a) Dependence on the distance of the ionization position from the skimmer in which the skimmer-cone distance was maintained to be 6.5 mm. (b) Dependence on the distance of the ionization position from the iron cone while maintaining the distance between the ionization point and the skimmer to be 2 mm. Broken lines are the expectation values calculated using the work functions of C (5.0 V) and Al (4.17 V) and assuming that the local work function varies linearly between the skimmer and the magnet. 4.17 eV is an average of the eBE values for three different Al-crystal orientations.[39] The photon energy is 21.7 eV.

cone attached to the magnet was separated by 6.5 mm from the entrance skimmer for the TOF spectrometer. The photoionization position was varied between the cone and the skimmer. In order to exclude any electrostatic influence of the graphite-coated gas nozzle, it was placed 10 mm away from the ionization point. As shown in Fig. 3(a), we confirmed that PKE was independent of the ionization position when the iron cone was coated with graphite. On the other hand, when the cone was wrapped with an Al foil, PKE shifted systematically due to the difference of work functions between the graphite and Al. We also performed a different type of experiment in which the ionization position was fixed at 2 mm from the graphite-coated skimmer and the position of the iron cone was shifted gradually with respect to the ionization position. As shown in Fig. 3(b), PKE was almost invariant with the position of the graphite-coated cone, while PKE clearly shifted with the position of the Al-wrapped cone. Similar experiments performed using the $1b_1$ band of gaseous water evaporated from the liquid microjet of aqueous 30 mM NaBr solution revealed the same behavior, as shown in Fig. 4.

Next, we examined the influence of the gas nozzle by measuring PKE as a function of the height of the nozzle from the ionization point. The distances among the ionization point, skimmer, and iron cone were maintained to be the same. Figure 5 shows the results thus obtained with Xe. The red dot and blue triangle show the cases of the graphite-coated and Al-wrapped iron cone, respectively. When the graphite-coated cone was employed, PKE was independent of

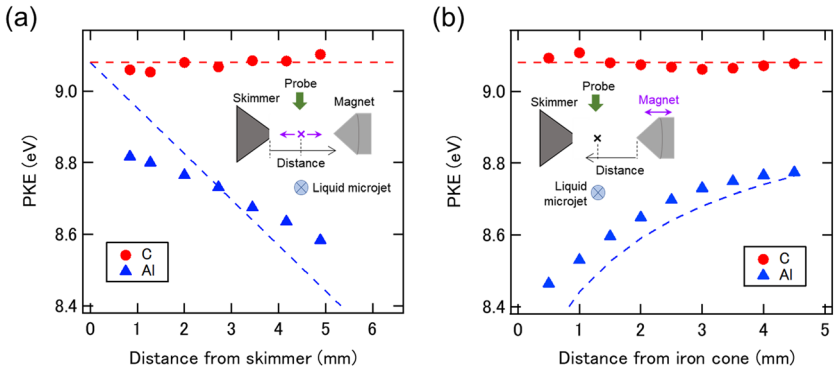

FIG. 4. Similar results with Fig. 3 obtained using the $1b_1$ photoelectron band of gaseous water. The inset shows the experimental geometries. The gaseous water is supplied by thermal evaporation from the liquid microjet surface of aqueous 30 mM NaBr solution discharged from a graphite-coated silica capillary with the 25-μm inner diameter and the flow rate of 0.5 ml/min. The liquid microjet is placed more than 8 mm away from the ionization position along the XUV laser propagation direction. Red dots are the results obtained with a carbon-coated iron cone on a SmCo magnet and blue triangles are those obtained with an Al-wrapped iron cone. (a) Dependence on the distance of the ionization point (indicated by cross) from the skimmer while maintaining the skimmer-cone distance to be 6.5 mm. (b) Dependence on the distance between the ionization point and the iron cone while maintaining the distance between the ionization point and the skimmer to be 2 mm. Broken lines are the expectation when the local work function varies linearly between the skimmer and the magnet. The photon energy is 21.7 eV.

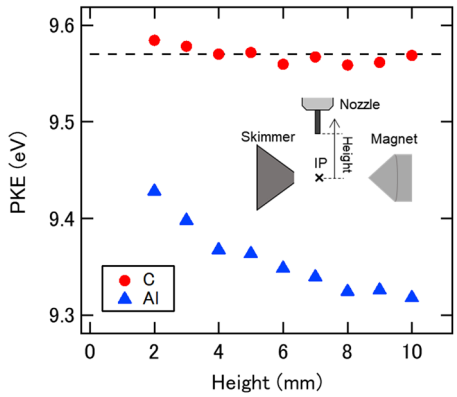

FIG. 5. Influence of the distance between the gas nozzle and the ionization position (indicated by cross) upon PKE of Xe. The inset shows the experimental geometry. The ionization position and the cone are fixed at 2 mm and 6.5 mm from the skimmer, respectively. Red dots and blue triangles are the results measured with a graphite-coated and Al-wrapped iron cone, respectively. Dashed line shows the PKE expected for the correct eBE of Xe. The photon energy is 21.7 eV.

the height of a gas nozzle, as anticipated. On the other hand, PKE changed with the nozzle position when using the Al-wrapped cone; as the graphite-coated nozzle approaches the ionization point, PKE gradually increased.

III. DEPENDENCES OF Φ_{surf} ON VARIOUS PARAMETERS

A. NaX concentration

Kurahashi *et al.* and Preissler *et al.* measured the streaming current for aqueous NaI solution at various concentrations using a liquid microjet discharged from fused silica capillaries.[22,23] Both found a positive streaming current at low concentrations and a negative current at high concentrations. Correspondingly, PKE monotonically increased with the concentration for both chemical species in the gas phase and in solution. In the present study, we estimated Φ_{surf} as a function of NaI concentration using the $1b_1$ band of gaseous water with the XUV-MBTOF spectrometer, as shown in Fig. 6. One can see that Φ_{surf} is reversed from the positive to negative value near the concentration of 30 mM and PKE increases with the NaX concentration, in agreement with the previous study.[22] Thus, we confirmed that Φ_{surf} diminishes monotonically with the NaX concentration. Kurahashi *et al.* found that, when using a flat aperture for their hemispherical electron energy analyzer, the PKE shift occurred in the opposite direction from the expectation. In the present study, we confirmed that the direction of the PKE shift with the NaX concentration is the same for a graphite-coated aperture or a graphite-coated skimmer placed at the entrance of our MBTOF apparatus. Furthermore, the direction of the shift was confirmed to be the same for a linear TOF spectrometer without the permanent magnet. It remains unclear why the energy shift appeared oppositely in the experiment by Kurahashi *et al.*,[22] however, they have correctly identified the polarity by comparison with the streaming current measurements[22] so that their final conclusion was the same with the present study.

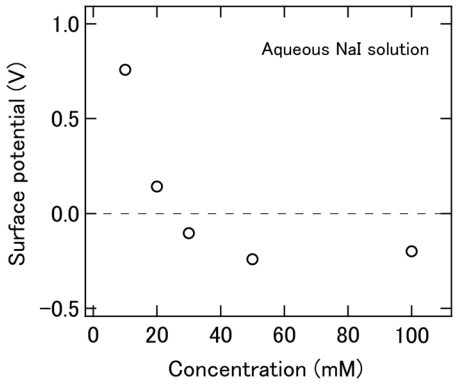

FIG. 6. Concentration dependence of Φ_{surf} determined by the $1b_1$ valence band of gaseous water measured using the 29.45 eV probe photons.

B. Flow rate

Figure 7 shows Φ_{surf} measured as a function of a liquid flow rate. A 25-μm inner diameter fused silica capillary was used. It is seen that Φ_{surf} always increases (PKE diminishes) with the flow rate, irrespective of the polarity of Φ_{surf} at a low flow rate. The variation of Φ_{surf} is greater at lower concentration, and the rate of change diminishes at a higher concentration. When approximating the concentration dependence of Φ_{surf} to be linearly dependent on the flow rate, we may crudely estimate Φ_0 to be about −0.4 V.

Preissler *et al.* examined a streaming current, using a method similar to that of Holstein *et al.*,[20] as a function of the flow rate from 0.2 ml/min to 0.6 ml/min using a 15-μm inner diameter fused silica capillary: owing to the difference of the inner diameter of capillaries, their jet velocity was higher by 2.8 times than ours at the same flow rate.[23] They found that the overall charge of a microjet changes into the positive direction for higher flow rate at all concentrations (1–500 mM) of the aqueous NaI solution, which is consistent with the monotonic increase of Φ_{surf} with the flow rate observed in the present study. Preissler *et al.* argued that the estimated

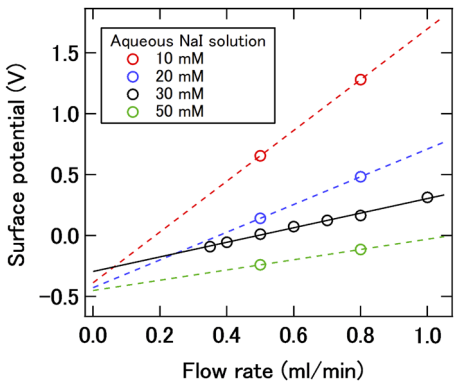

FIG. 7. Flow rate dependence of the surface potential determined using the $1b_1$ valence band of gaseous water measured using 29.45 eV photons. The solid line for 30 mM is the linear fit, and the broken lines are drawn as a guide for the eye.

surface potential of a liquid microjet is far smaller than that expected from the streaming current measured *in situ* in vacuum and that a large fraction of the measured streaming current arises from molecular ions, which evaporated from the jet surface and traveled along the jet direction.[23] They measured the jet diameter in vacuum to be 10 μm.

C. Temperature

We have noted that PKE slightly varies with the liquid temperature in a systematic manner. The liquid temperature we measured was prior to discharge from the nozzle. Although the temperature was varied only up to 293 K, the measured PKE of the $1b_1$ band of gaseous water clearly increased with the liquid temperature, as shown in Fig. 8(a), indicating that Φ_{surf} decreases with the temperature. The rate of change is greater for lower concentration of the electrolyte. The origin of this temperature dependence is not quite clear. However, it is noted that the viscosity of liquid water increases at lower temperature[40] so that the liquid pressure increases at lower temperature, as shown in Fig. 8(b), when a constant flow condition of 0.5 ml/min was maintained. Thus, the temperature dependence of Φ_{surf} is probably ascribed to the liquid pressure. Since the liquid pressure increases with the flow rate, the temperature and flow rate dependence are consistent with each other. The result indicates that accurate measurement requires a stable sample temperature and liquid pressure.

IV. INFLUENCE OF STATIC POTENTIAL APPLIED TO LIQUID DISCHARGING NOZZLE

A. XUV one-photon ionization

By applying an external DC voltage to the microjet, the vacuum level at the jet can be varied to make the electric potential around the microjet to be flat. However, it has not been clarified, as far as we noticed, whether this method provides the same effect with the adjustment of electrolyte concentration. Figure 9 shows PKE associated with the $1b_1$ band of gaseous water measured as a function of the distance from the liquid microjet of aqueous NaBr solution. Two different concentrations of (a) 1 mM and (b) 100 mM were examined. By analyzing the gradual change in PKE with the distance, indicated by red circles in Fig. 9, Φ_{surf} was estimated to be 1.82 V and −0.33 V for 1 mM and 100 mM, respectively. As the liquid microjet was moved away from the ionization point toward the magnet, the PKE value gradually approaches an asymptotic value indicated by the broken line. The asymptotic PKE value is very close to the true value calculated from the correct eBE, and the deviation (ΔE) from the true value is evaluated to be 0.00 ± 0.02 eV and −0.04 ± 0.01 eV for 1 mM and 100 mM, respectively. This is because the photoelectron spectrometer without the liquid microjet has already been calibrated with a standard gas, and the PKE value can be measured under negligible influence from the microjet.

Next, we applied an external voltage to the liquid discharging nozzle to flatten the vacuum level around the liquid microjet. In the case of 1 mM solution, the vacuum level could be flattened by applying −4 V to the nozzle; the rather large voltage is attributed to low electric conductivity of the liquid (0.16 mS/cm). The low conductivity caused an instability of PKE and a relatively large uncertainty in the estimated Φ_{surf}. The conductivity of 100 mM solution was as large as 12 mS/cm. After the vacuum level gradient was eliminated with the static voltage, Φ_{surf} estimated from the gradient of the potential was much reduced to 0.10 eV and 0.04 eV. On the other hand, the entire spectrum has shifted as much as ΔE = 1.48 ± 0.04 eV and −0.17 ± 0.01 eV for 1 mM and 100 mM solutions, respectively. The results indicate that one can apply an external voltage to make the local vacuum level of a microjet to be closer to that of graphite, while the voltage shifts the entire spectrum. The magnitude of this shift is in the same order

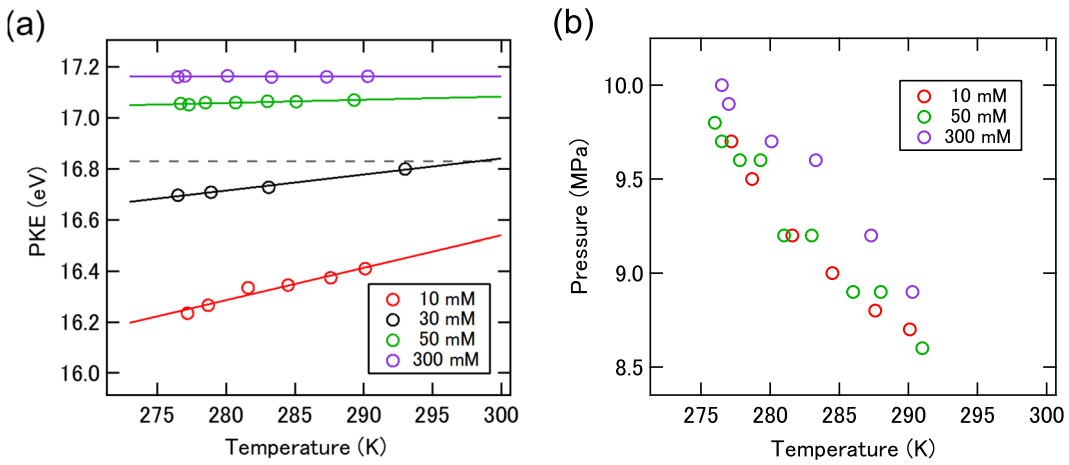

FIG. 8. (a) Temperature dependence of PKE associated with the $1b_1$ valence band of gaseous water measured using 29.45 eV photons. Water vapor is supplied from the NaI liquid microjet placed at the 300 μm away from the ionization point. The solid lines for each concentration plot are linear fits. Dashed line indicates the expected PKE of the $1b_1$ valence band. (b) Temperature dependence of the liquid pressure by HPLC pump with various concentrations of aqueous NaI solution.

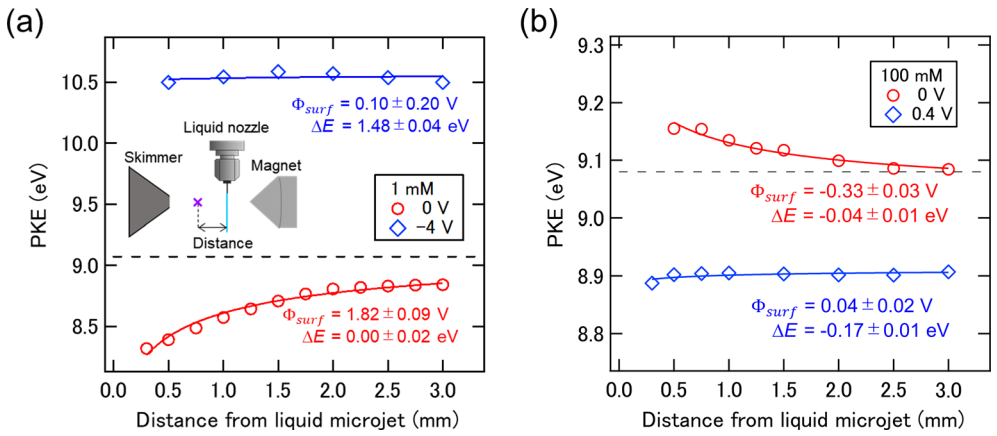

FIG. 9. PKE of the $1b_1$ valence band of gaseous water measured as a function of the distance between the ionization point and the liquid microjet of aqueous NaBr solution at the concentrations of (a) 1 mM and (b) 100 mM. The inset shows the experimental geometry. The ionization point (indicated by cross) is fixed at 2 mm from the skimmer. The probe photon energy is 21.7 eV. Red circles and blue diamonds show PKE observed with and without the external DC voltage, respectively. Dashed line indicates the expected PKE of the $1b_1$ valence band. The solid lines are the least squares fits using the equation reported by Kurahashi *et al.*[22]

with the applied voltage. The result indicates that energy recalibration is indispensable after the external voltage is applied to the nozzle.

For further clarifying the variation of Φ_{surf} and ΔE with the voltage, Figs. 10(a) and 10(b) show Φ_{surf} and ΔE, respectively, determined for the aqueous 50 mM NaBr solution as a function of an applied voltage. Both quantities vary linearly. The potential gradient can be eliminated at a certain voltage, whereas the entire shift of the spectrum vanishes at a different voltage. Thus, PKE must be calibrated using a reference sample when using a static voltage to flatten the potential around the microjet.

B. Multiphoton ionization with UV radiation

Similar to the experiment described in Sec. IV A, we measured PKE for multiphoton ionization of a reference gas with UV light. The experimental geometry is shownin Fig. 11. PKE of NO was measured using [1 + 1] resonance-enhanced multiphoton ionization (REMPI) via the A state at 226 nm, and the position of liquid microjet was varied with respect to the fixed ionization point. Figure 12 shows an example of such measurements using the aqueous 0.1M NaI solution. The liquid discharging nozzle was a graphite-coated silica capillary with a 25-μm inner diameter and the flow rate was 0.5 ml/min. The photoelectron spectra measured as a function of the nozzle position indicates that PKE ultimately converges to 1.82 eV, which is shifted by 0.07 eV from the value measured in the absence of the liquid microjet.

Then, we applied an external DC voltage to the liquid microjet to flatten the vacuum level around the jet and calibrated the entire spectrum using photoionization of gaseous NO. The method has been employed already in our study on aqueous TBAI solutions.[41] Figure 13 shows the PKE measured for NO as a function of the distance from the microjet of aqueous NaI solution discharged from a

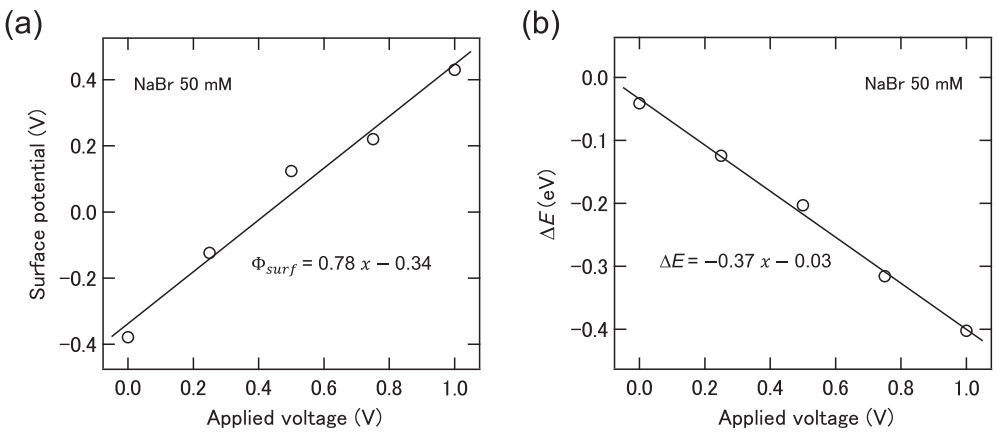

FIG. 10. The applied voltage dependences of (a) Φ_{surf} and (b) ΔE using the liquid microjet of aqueous NaBr solution at 50 mM. Solid lines are the linear fits.

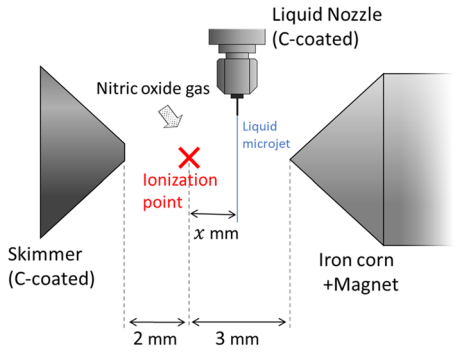

FIG. 11. Experimental geometry to estimate the surface potential of the liquid microjet. The skimmer with 0.5 mm hole and the liquid nozzle using a fused silica capillary with a 15-μm or 25-μm inner diameter are coated with graphite. An iron cone, without a graphite coat in this particular experiment, is placed on the samarium–cobalt magnet. Nitric oxide gas is introduced near the ionization point through a PEEK tube with 400 μm inner diameter.

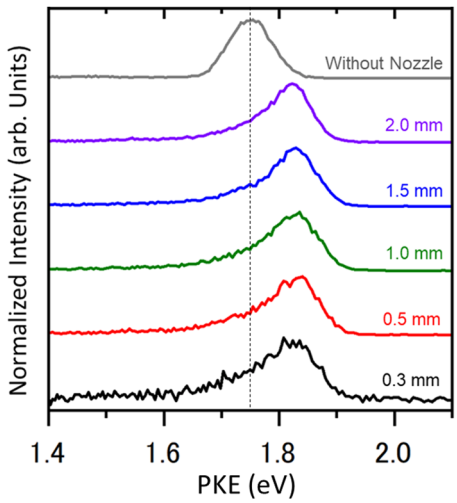

FIG. 12. Photoelectron spectra of nitric oxide gas measured by varying the nozzle position. Dashed line shows PKE observed without the liquid nozzle. The liquid microjet of aqueous NaI solution with 100 mM is discharged from a graphite-coated silica capillary with a 25-μm inner diameter, and the flow rate is 0.5 ml/min.

graphite-coated silica capillary with a 15-μm inner diameter at the flow rate of 0.2 ml/min. Two concentrations of (a) 10 mM and (b) 50 mM were examined. At 10 mM, Φ_{surf} was too large to measure and was presumably greater than 2 eV. By applying the static voltage of −1.9 V, we reduced the potential gradient and measured the photoelectron spectrum. ΔE was estimated to be 0.46 eV. For obtaining a stable liquid beam condition, a concentration higher than 10 mM was needed, at which the electric conductivity was greater than 1.5 mS/cm. At 50 mM, Φ_{surf} was estimated to be −0.11 V without the DC voltage, and application of 0.16 V to the nozzle eliminated the potential gradient, while ΔE of −0.05 eV remained. The dependence of Φ_{surf} and ΔE on the applied voltage shown in Fig. 14 is very similar to that in Fig. 10.

Previously, Olivieri *et al.*[27] measured eBE of the O(1s) orbital of gaseous water around the liquid microjet of an aqueous 50 mM NaCl solution by varying the external voltage to the liquid microjet. They found that the O(1s) bandwidth of gaseous water became narrowest when 0.5 V was applied to the microjet, implying that the vacuum level potential became flat within the ionization volume defined by the spatial distributions of excitation light and water vapor. Without the applied voltage, the eBE value of gaseous water differed from the literature value by 0.60 ± 0.07 eV. They argued that these values are consistent each other. However, based on their analysis, we find that deviation of an applied voltage from the optimum value by 0.1 V should cause an error of 0.07 eV in the estimated eBE. The magnitude of this error is in reasonable agreement with ΔE shown in Figs. 9(b) and 13(b). Olivieri *et al.* have noted that the fitting procedure was noticeably less reproducible under high voltage because the peak becomes exceedingly broad and weak, which restricted their discussion to small bias voltage. We conclude that the method of applying external bias to a liquid microjet is effective in flattening the potential around the microjet; however, the absolute energy scale must be recalibrated after applying the external voltage. This was clearly demonstrated in our study because we investigated aqueous solutions at very low electrolyte concentrations (1 mM and 10 mM), which revealed successful flattening of the vacuum energy around the microjet but a non-negligible energy shift (ΔE) from the true PKE value. When we employ a variable potential

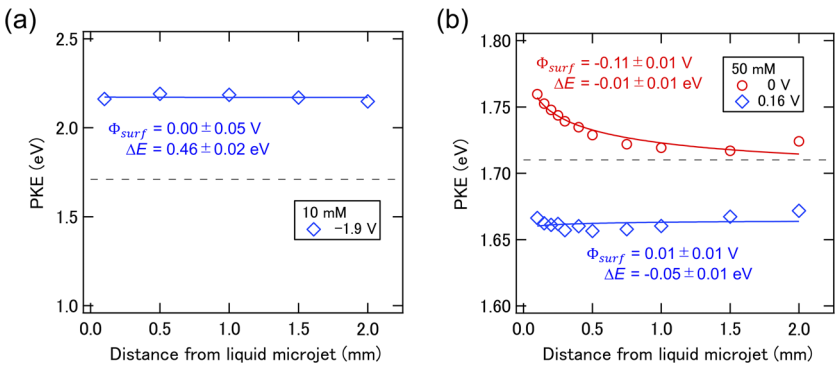

FIG. 13. PKE measured for nitric oxide as a function of the distance between the ionization point and the liquid microjet of aqueous NaI solution. The concentrations were (a) 10 mM and (b) 50 mM. The probe wavelength was 226 nm. Red circles and blue diamonds show PKE observed with and without the external DC voltage, respectively. Dashed line indicates the expected PKE. The solid lines are the least squares fits using the equation reported by Kurahashi *et al.*[22]

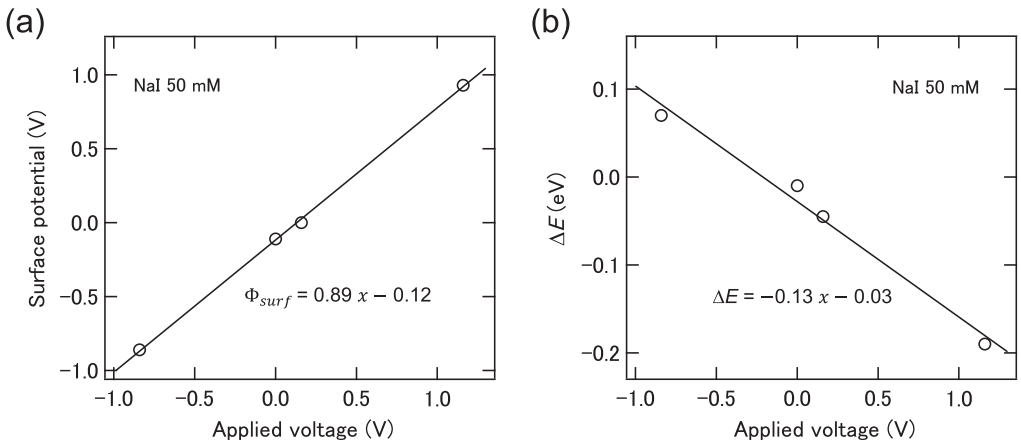

FIG. 14. The applied voltage dependences of (a) Φ_{surf} and (b) ΔE using the liquid microjet of aqueous NaI solution at 50 mM. Solid lines are the linear fits.

of a liquid microjet in our laboratory, we first find the voltage that makes PKE of the gaseous sample to be independent of the distance between the ionization point and a liquid microjet and then calibrate the spectrometer using at least two flight times. In the case of UV–UV TRPES, one can use one-color and two-color photoionization of NO as one of the convenient choices of the energy standards. Our results indicate that a greater error can occur at lower or higher sample concentrations if the energy shift of the entire spectrum after application of the bias voltage is not determined using a standard gas sample.

Perry *et al.*[33] performed an experiment similar to that by Olivieri *et al.*[27] and they measured photoelectron spectra of gaseous water around aqueous 50 mM NaCl solution to find the narrowest bandwidth at the applied voltage of 0.6 V. The inner diameter of the capillary was 25 μm and the flow rate was 0.35 ml/min, which are very similar to our experimental condition. The entrance skimmer in their case seems to be gold-coated. They found that the eBE of gaseous water to be 12.65(9) eV, in excellent agreement with the literature value 12.62 eV, at the applied voltage of 0.6 V. They claim that the method applying a tunable bias voltage to a microjet enables compensation of electrokinetic charging and the vacuum level offset simultaneously and that it is broadly applicable to other systems. However, we point out that 50 mM NaCl concentration employed by Olivieri *et al.*[27] and Perry *et al.*[33] is close to the singular point of 30 mM concentration reported by Kurahashi *et al.*,[22] and as we demonstrated in the present work, the entire spectral shift by the application of an external voltage could be as small as the experimental error. Thus, this is likely to be a rather special experimental condition.

With their method, Perry *et al.* have revised the vertical ionization energy of liquid water to be 11.67(15) eV, which is 0.4 eV higher than the previously estimated values.[22,34,35] Close examination of their calibration method [Fig. 4(b) of their paper] reveals that an experimental uncertainty on the order of 0.1 eV possibly remains, similar to that in the work of Olivieri *et al.*[27] However, the 0.4 eV correction for the vertical ionization energy of liquid water is greater than a possible error in the calibration method we expect for their experimental condition. At this point, the origin of the 0.4 eV difference from the previous measurements remains unclear.

In general, calibration of a time-of-flight photoelectron energy analyzer needs at least two different electron flight times for accurate PKEs calculated from the photon energy and accurate eBE. In the case of XUV-TRPES, Xe atom can be a convenient reference gas because the doublet of $^2P_{3/2}$ (12.130) and $^2P_{1/2}$ (13.436) eV is clearly resolved with the energy resolution (0.38 eV) of our instrument (an electron spectrometer and ultrafast lasers). On the other hand, the photoelectron spectrum of Ar provides peaks at 15.759 eV and 15.937 eV, which are not resolved with our instrument. Perry *et al.* described that they calibrated their spectrometer using Ar and liquid water.[33] The brief description of their experimental condition does not enable us to know the actual procedure; however, calibration of the spectrometer is certainly crucial for the accuracy of measurements. Precise measurement of the photon energy is also important; Perry *et al.* have determined the photon energy down to the second place after the decimal so that this factor is well defined in their experiment. Previous measurements of eBE of liquid water were performed using soft x-ray radiation at the third generation synchrotron radiation facilities using hemispherical electron energy analyzers; the experiment by Nishizawa *et al.* was performed at the overall instrumental resolution of 0.1 eV.[35] At this stage, our own measurements of the vertical ionization energy of liquid water are negative to the suggested value greater than 11.4 eV.

Thus, while the 0.4 eV correction is important, its origin remains unclear. Another interesting feature we noted is that Perry *et al.* indicated that the bias voltage required for obtaining the narrowest bandwidth of gaseous water increases with the liquid flow rate.[33] This implies that the liquid becomes more negatively charged at a higher flow rate, which is an opposite trend observed in the present (Fig. 7) and previous studies.[22,23] The reason for this contradiction is also unclear, but it might provide more insights into the origin of 0.4 eV correction.

V. CONCLUSION

With the graphite-coated vacuum components, a magnetic bottle time-of-flight photoelectron spectrometer ensures accurate measurements of the photoelectron kinetic energy. However, when a liquid microjet is introduced, the work function and actual electric charges of the microjet influence the vacuum level around the jet and alter photoelectron kinetic energies measured for the liquid itself and surrounding gases. For reliable calibration of the energy, it is desirable to minimize the difference of vacuum levels between the liquid and graphite. This is possible by adjusting the electrolyte concentration and/or applying an external voltage to the liquid discharging nozzle. Even in the latter case, a certain amount of electrolyte is necessary for stabilizing the electric potential of the liquid microjet; a practical guideline for the conductivity of liquid is 1 mS/cm, which corresponds to about 10 mM of NaX. An external voltage applied to the microjet flattens the potential around it but shifts the potential entirely with respect to the vacuum level of the analyzer. Thus, energy calibration using a standard gas sample is indispensable after minimizing the vacuum potential gradient. In addition to the energy calibration of the spectrometer, the temperature and flow rate of a microjet must be stabilized for accurate measurements.

ACKNOWLEDGMENTS

The authors thank A. Hara and S. Kudo for their experimental assistance in the early stage of this work. This work was supported by JSPS KAKENHI (Grant No. 15H05753). C. W. West was supported by a Research Fellowship P16036 awarded by the Japan Society for the Promotion of Science.

The data that support the findings of this study are available within the article.

REFERENCES

[1] M. Faubel, in *Photoionization and Photodetachment*, edited by C.-Y. Ng (World Scientific, 2000).
[2] B. Winter and M. Faubel, Chem. Rev. **106**, 1176 (2006).
[3] P. Jungwirth and B. Winter, Annu. Rev. Phys. Chem. **59**, 343 (2008).
[4] R. Seidel, S. Thürmer, and B. Winter, J. Phys. Chem. Lett. **2**, 633 (2011).
[5] M. Faubel, K. R. Siefermann, Y. Liu, and B. Abel, Acc. Chem. Res. **45**, 120 (2012).
[6] R. Seidel, B. Winter, and S. E. Bradforth, Annu. Rev. Phys. Chem. **67**, 283 (2016).
[7] T. Suzuki, Int. Rev. Phys. Chem. **31**, 265 (2012).
[8] T. Suzuki, J. Chem. Phys. **151**, 090901 (2019).
[9] K. R. Siefermann, Y. Liu, E. Lugovoy, O. Link, M. Faubel, U. Buck, B. Winter, and B. Abel, Nat. Chem. **2**, 274 (2010).
[10] Y. Tang, H. Shen, K. Sekiguchi, N. Kurahashi, T. Mizuno, Y.-I. Suzuki, and T. Suzuki, Phys. Chem. Chem. Phys. **12**, 3653 (2010).
[11] A. Lübcke, F. Buchner, N. Heine, I. V. Hertel, and T. Schultz, Phys. Chem. Chem. Phys. **12**, 14629 (2010).
[12] M. H. Elkins, H. L. Williams, A. T. Shreve, and D. M. Neumark, Science **342**, 1496 (2013).
[13] H. Tissot, J.-J. Gallet, F. Bournel, G. Olivieri, M. G. Silly, F. Sirotti, A. Boucly, and F. Rochet, Top. Catal. **59**, 605 (2016).
[14] N. Engel, S. I. Bokarev, A. Moguilevski, A. A. Raheem, R. Al-Obaidi, T. Möhle, G. Grell, K. R. Siefermann, B. Abel, S. G. Aziz, O. Kühn, M. Borgwardt, I. Y. Kiyan, and E. F. Aziz, Phys. Chem. Chem. Phys. **19**, 14248 (2017).
[15] J. Ojeda, C. A. Arrell, L. Longetti, M. Chergui, and J. Helbing, Phys. Chem. Chem. Phys. **19**, 17052 (2017).
[16] I. Jordan, A. Jain, T. Gaumnitz, J. Ma, and H. J. Wörner, Rev. Sci. Instrum. **89**, 053103 (2018).
[17] J. Hummert, G. Reitsma, N. Mayer, E. Ikonnikov, M. Eckstein, and O. Kornilov, J. Phys. Chem. Lett. **9**, 6649 (2018).
[18] J. W. Riley, B. Wang, J. L. Woodhouse, M. Assmann, G. A. Worth, and H. H. Fielding, J. Phys. Chem. Lett. **9**, 678 (2018).
[19] M. Faubel and B. Steiner, Ber. Bunsenges. Phys. Chem. **96**, 1167 (1992).
[20] W. L. Holstein, L. J. Hayes, E. M. C. Robinson, G. S. Laurence, and M. A. Buntine, J. Phys. Chem. B **103**, 3035 (1999).
[21] Y. Tang, Y.-i. Suzuki, H. Shen, K. Sekiguchi, N. Kurahashi, K. Nishizawa, P. Zuo, and T. Suzuki, Chem. Phys. Lett. **494**, 111 (2010).
[22] N. Kurahashi, S. Karashima, Y. Tang, T. Horio, B. Abulimiti, Y.-I. Suzuki, Y. Ogi, M. Oura, and T. Suzuki, J. Chem. Phys. **140**, 174506 (2014).
[23] N. Preissler, F. Buchner, T. Schultz, and A. Lübcke, J. Phys. Chem. B **117**, 2422 (2013).
[24] N. Kurahashi and T. Suzuki, Chem. Lett. **47**, 16 (2018).
[25] A. Henley, J. W. Riley, B. Wang, and H. H. Fielding, Faraday Discuss. **221**, 202 (2020).
[26] M. Faubel, B. Steiner, and J. P. Toennies, J. Chem. Phys. **106**, 9013 (1997).
[27] G. Olivieri, A. Goel, A. Kleibert, D. Cvetko, and M. A. Brown, Phys. Chem. Chem. Phys. **18**, 29506 (2016).
[28] P. Kruit and F. H. Read, J. Phys. E: Sci. Instrum. **16**, 313 (1983).
[29] K. Müller-Dethlefs, M. Sander, and E. W. Schlag, Chem. Phys. Lett. **112**, 291 (1984).
[30] K. Muller-Dethlefs and E. W. Schlag, Annu. Rev. Phys. Chem. **42**, 109 (1991).
[31] A. P. Gaiduk, M. Govoni, R. Seidel, J. H. Skone, B. Winter, and G. Galli, J. Am. Chem. Soc. **138**, 6912 (2016).
[32] M. N. Pohl, E. Muchová, R. Seidel, H. Ali, Š. Sršeň, I. Wilkinson, B. Winter, and P. Slavíček, Chem. Sci. **10**, 848 (2019).
[33] C. F. Perry, P. Zhang, F. B. Nunes, I. Jordan, A. von Conta, and H. J. Wörner, J. Phys. Chem. Lett. **11**, 1789 (2020).
[34] B. Winter, R. Weber, W. Widdra, M. Dittmar, M. Faubel, and I. V. Hertel, J. Phys. Chem. A **108**, 2625 (2004).
[35] K. Nishizawa, N. Kurahashi, K. Sekiguchi, T. Mizuno, Y. Ogi, T. Horio, M. Oura, N. Kosugi, and T. Suzuki, Phys. Chem. Chem. Phys. **13**, 413 (2011).
[36] J. Nishitani, C. W. West, and T. Suzuki, Struct. Dyn. **4**, 044014 (2017).
[37] J. Nishitani, Y.-i. Yamamoto, C. W. West, S. Karashima, and T. Suzuki, Sci. Adv. **5**, eaaw6896 (2019).
[38] J. W. Riley, B. Wang, M. A. Parkes, and H. H. Fielding, Rev. Sci. Instrum. **90**, 083104 (2019).
[39] D. R. Lide, *CRC Handbook of Chemistry and Physics*, 85th ed. (CRC Press, 2004).
[40] J. Kestin, M. Sokolov, and W. A. Wakeham, J. Phys. Chem. Ref. Data **7**, 941 (1978).
[41] S. Karashima and T. Suzuki, J. Phys. Chem. B **123**, 3769 (2019).